CRYSTAL GROWTH & DESIGN

Communication

Cite This: *Cryst. Growth Des.* 2019, 19, 2511−2518

pubs.acs.org/crystal

Application of Long-Range Synthon Aufbau Modules Based on Trihalophenols To Direct Reactivity in Binary Cocrystals: Orthogonal Hydrogen Bonding and $\pi-\pi$ Contact Driven Self-Assembly with Single-Crystal Reactivity

Published as part of the Crystal Growth and Design Israel Goldberg Memorial virtual special issue

Gonzalo Campillo-Alvarado, Changan Li, Dale C. Swenson, and Leonard R. MacGillivray*

Department of Chemistry, University of Iowa, Iowa City, Iowa 52242, United States

Supporting Information

ABSTRACT: The ability of 2,4,6-trihalophenols (**3X-phOH**) (where X = F, Cl, or Br) to enable reactivity of 1,2-bis(4-pyridyl)ethylene (**bpe**) in the solid state via cocrystallization is reported. The trihalophenols display structure behavior defined by infinite face-to-face $\pi\cdots\pi$ contacts and hydrogen bonds as pure solids that we show can be transferred to binary cocrystals to organize **bpe** to undergo a solid-state photodimerization. Cocrystals based on Cl- and Br-halophenols undergo single-crystal-to-single-crystal photoreactions to afford *rctt*-tetrakis(4-pyridyl)cyclobutane (**tpcb**) stereoselectively and in near quantitative yield. The use of **3X-phOH** to enable reactivity in the solid state is discussed in the context of long-range synthon Aufbau modules.

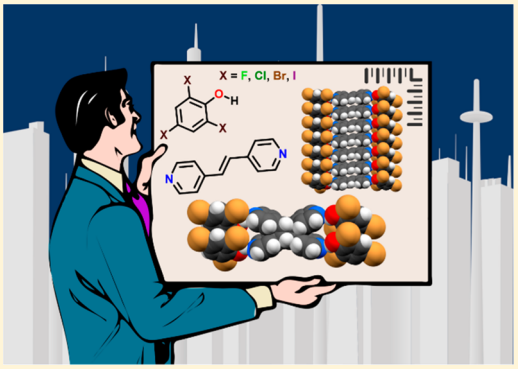

Ganguly and Desiraju have recently introduced the concept of long-range synthon Aufbau modules (LSAMs) as a means to influence and control the packing of molecules in organic solids.[1] The approach relies on identifying long-range supramolecular synthons that make up parts of crystal structures and ultimately transferring those LSAMs to related chemical systems to control the three-dimensionality (3D) of a structure.[2−10]

As part of our efforts to utilize principles of supramolecular chemistry to control photoreactivity in organic solids,[11−14] we report here the identification and ability of an LSAM based on a series of 2,4,6-trihalophenols to direct a [2 + 2] photodimerization in the solid state (Scheme 1). The LSAMs are defined by one-dimensional (1D) face-to-face π-stacking of the trihalophenols observed in the pure solid forms that we show can be transferred to binary cocrystals to assemble an alkene to undergo an intermolecular [2 + 2] photodimerization. Specifically, we demonstrate the ability of LSAMs of 2,4,6-trihalophenols (**3X-phOH**) (where X = F, Cl, Br, or I) to assemble 1,2-bis(4-pyridyl)ethylene (**bpe**) into 1D π-stacks via O−H···N hydrogen bonds in cocrystals of composition 2(**3X-phOH**)·(**bpe**) to react to afford *rctt*-tetrakis(4-pyridyl)-cyclobutane (**tpcb**) stereoselectively and in near quantitative yield (for X = F, Cl, Br). For **3Cl-phOH** and **3Br-phOH**, the photodimerizations proceed as rare single-crystal-to-single-crystal transformations (SCSC).[15] We are unaware of an example wherein the concept of an LSAM has been exploited to direct a chemical reaction in a solid.[16]

Experimental. Cocrystal Syntheses and Photochemical Studies. Methanol (solvent) and **bpe** were purchased from Sigma-Aldrich, **3F-phOH** was purchased from Alfa-Aesar, and **3Cl-phOH**, **3Br-phOH** and **3I-phOH** were purchased from TCI Chemicals. All chemicals were used as received without further purification. Cocrystals of 2(**3F-phOH**)·(**bpe**), 2(**3Cl-phOH**)·(**bpe**), 2(**3Br-phOH**)·(**bpe**), and 2(**3I-phOH**)·(**bpe**) were generated by dissolving the corresponding halophenol (0.20 mmol) and **bpe** (0.10 mmol) in warm methanol (3.0 mL). Single crystals were formed upon cooling each solution to room temperature and allowing each solution to sit for a period of approximately 2 days. Each single crystal sample was ground into a powder using an agate mortar-and-pestle and then placed between two Pyrex glass plates. Photoreactions were conducted using UV-radiation from a 450 W medium-pressure mercury lamp in an ACE Glass photochemistry cabinet. Single-crystal-to-single-crystal transformations were conducted by UV-irradiating single crystals in a UV light gel nail dryer for 48 h.[17] The progress of each photoreaction was monitored using ^{1}H NMR spectroscopy.

X-ray Crystallography. Single-crystal X-ray diffraction (SCXRD) data were collected on Bruker Nonius APEX II Kappa and Nonius Kappa CCD single-crystal X-ray diffractometers using Mo$K\alpha$ radiation (λ = 0.71073 Å). Crystals were

Received: January 8, 2019
Revised: February 28, 2019
Published: March 20, 2019

DOI: 10.1021/acs.cgd.9b00035
Cryst. Growth Des. 2019, 19, 2511−2518

Scheme 1. Trihalophenol Assemblies: (a) LSAM (Pink) Defined by One-Dimensional Face-to-Face π-Stacking of 3X-phOH as Pure Forms for (a) X = Cl, I[a] and (b) X = F, Cl, Br, and I and (c) Transferability of LSAM To Direct a [2 + 2] Photodimerization of bpe to Form tpcb

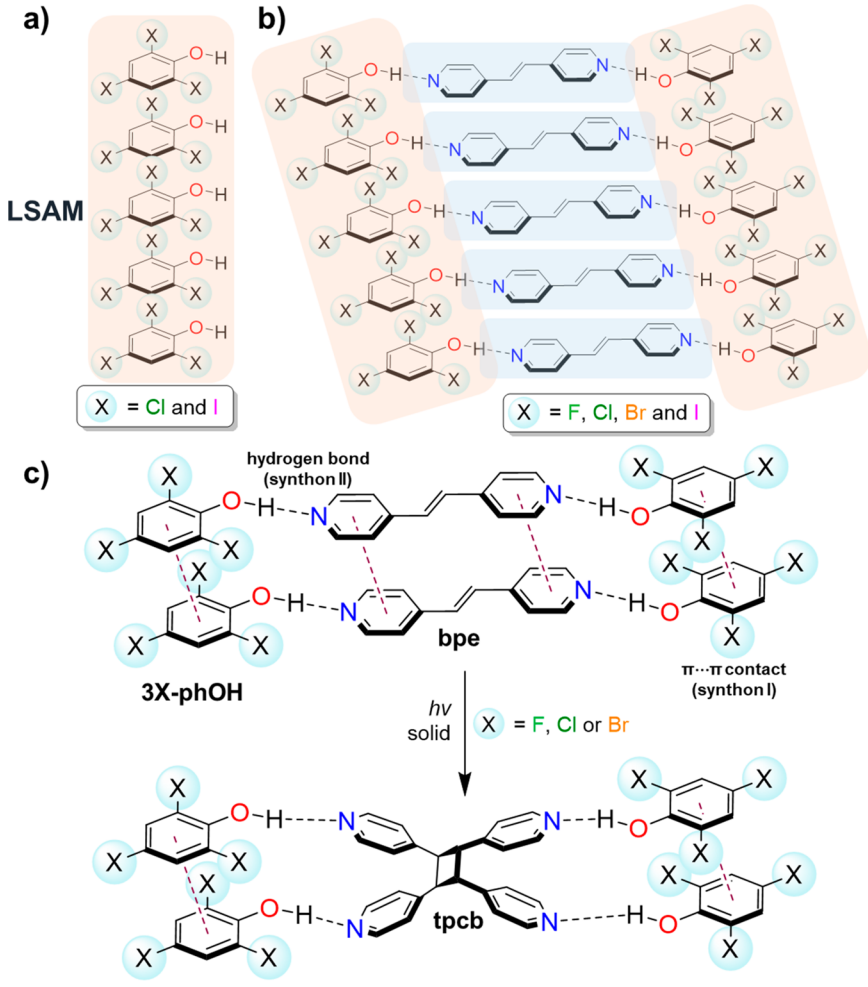

[a]Note directionality of −OH groups.

Table 1. X-ray Crystallographic Data for 2(3F-phOH)·(bpe), 2(3Cl-phOH)·(bpe), 2(3Br-phOH)·(bpe), and 2(3I-phOH)·(bpe)

crystal data[a]	2(3F-phOH)·(bpe)	2(3Cl-phOH)·(bpe)	2(3Br-phOH)·(bpe)	2(3I-phOH)·(bpe)
chemical formula	$2(C_6H_3F_3O)\cdot C_{10}H_8N_2$	$2(C_6H_3Cl_3O)\cdot C_{10}H_8N_2$	$2(C_6H_3Br_3O)\cdot C_{10}H_8N_2$	$2(C_6H_3I_3O)\cdot C_{10}H_8N_2$
MW (g mol^{-1})	464.45	563.17	829.89	1111.89
space group	$P\bar{1}$	$P2_1/c$	$P2_1/n$	$P2_1/c$
a (Å)	3.7344(4)	14.1588(14)	4.0371(4)	4.3124(4)
b (Å)	12.9484(13)	3.9749(4)	26.040(3)	12.7537(13)
c (Å)	21.544(2)	21.837(2)	12.3632(12)	26.046(3)
α (deg)	95.280(5)	90	90	90
β (deg)	94.210(5)	90.479(5)	93.358(5)	91.532(5)
γ (deg)	91.647(5)	90	90	90
V (Å^3)	1033.87(18)	1228.9(2)	1297.5(2)	1432.0(3)
Z	2	4	2	2
μ (mm^{-1})	0.135	0.726	9.309	6.532
ρ_{calcd} (g cm^{-3})	1.537	1.560	2.160	2.611
R_1[b,c]	0.0488	0.0298	0.0456	0.0311
wR_2[d,e]	0.1156	0.0799	0.0892	0.0549
CCDC	1883873	1883874	1883875	1883876

[a]$\lambda_{MoK\alpha}$ = 0.71073 Å. [b]$F_0 > 2\sigma(F_0)$. [c]$R_1 = \sum||F_0| - |F_c||/\sum|F_0|$. [d]All data. [e]$wR_2 = [\sum w(F_0^2 - F_c^2)^2/\sum w(F_0^2)^2]^{1/2}$.

DOI: 10.1021/acs.cgd.9b00035
Cryst. Growth Des. 2019, 19, 2511−2518

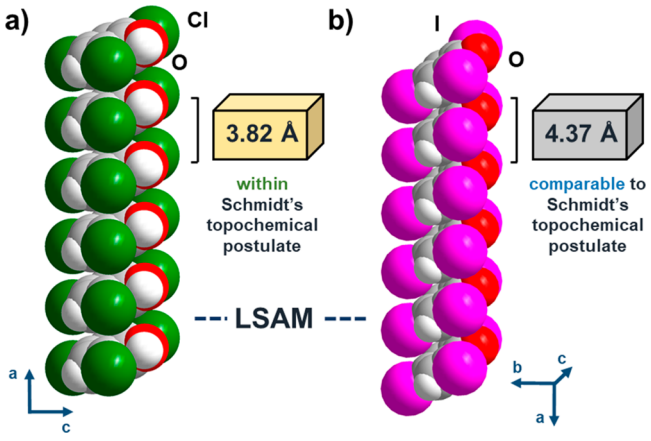

Figure 1. X-ray structures of pure **3X-phOH** showing LSAMs: (a) X = Cl and (b) X = I.[26,27]

mounted in Paratone oil on a Mitegen magnetic mount. Lorentz and polarization corrections were applied, and programs from the APEXII package were used for data reduction. Structure solution and refinement were performed using SHELXT[18] and SHELXL,[19] respectively within the Olex2[20] and WinGX[21] graphical user interfaces. Crystallographic data for cocrystals are summarized in Table 1. Powder X-ray diffraction (PXRD) data were collected on a Bruker D8 Advance X-ray diffractometer using CuKα1 radiation (λ = 1.5418 Å) typically in the range of 5−40° 2θ (scan type: coupled TwoTheta/Theta; scan mode: continuous PSD fast; step size: 0.019°) (40 kV and 30 mA).

Results and Discussion. Rationale toward Design. Halophenols are present in marine environments[22] and widely used in the manufacturing of pesticides and wood preservatives.[23] From a crystal engineering perspective, halophenols have contributed to define the term "halogen bond",[24] serving as building blocks in molecular recognition and self-assembly.[3,5,16] Halophenols have also recently presented opportunities to influence mechanical behaviors of solids (i.e., plastic deformation) owing to combinations of noncovalent forces (i.e., hydrogen bonds, halogen bonds, π-stacking) being propagated in orthogonal directions.[16,25]

Our efforts to utilize cocrystals based on **3X-phOH** to enable photoreactivity of **bpe** is inspired by work of Desiraju who demonstrated a propensity of related 3,4,5- and 2,3,4-trichlorophenols to assemble in the solid state with anilines by a combination of face-to-face $\pi\cdots\pi$ contacts and hydrogen bonds. The forces were propagated in 2D forming long-range and higher-order aggregates with components in arrangements that were shown to be transferrable to cocrystals of aniline derivatives.[5,6] The work of Desiraju prompted us to explore the potential to employ **3X-phOH** to direct an intermolecular [2 + 2] photodimerization of **bpe**.

Specifically, examinations of the X-ray structures of **3X-phOH** (CSD Refcodes: SILGOK (X = Cl) and BOLNEW (X = I))[26,27] (Figure 1) as pure forms revealed the molecules to self-assemble in the solid state to form 1D face-to-face π-stacks (Figure 1a,b). For X = Cl, the molecules interact via face-to-face $\pi\cdots\pi$ contacts wherein the hydroxyl groups participate in O−H···O hydrogen bonds (Figure 1c). Importantly, the hydroxyl groups are oriented in the same direction along the peripheries of the 1D stacks and are separated by 3.82 Å. For X = I, the face-to-face $\pi\cdots\pi$ contacts are present, yet the hydroxyl groups do not participate in an O−H···O hydrogen bond. Instead, the hydroxyl groups, while also being oriented in the same directions, have H atoms that lie in close proximity to I atoms (Figure 1d). The hydroxyl groups are separated by 4.37 Å along the stacks. The solid-state structure for X = I is a rare example of a solid with essentially a "free" hydroxyl group.[28] Moreover, we hypothesized that the 1D packings of the trihalogenated phenols may be exploited as LSAMs whereby the π-stacking and hydroxyl group orientations are preserved and transferred to form binary cocrystals wherein the LSAMs direct face-to-face stacking of **bpe**. The infinite stacking of the

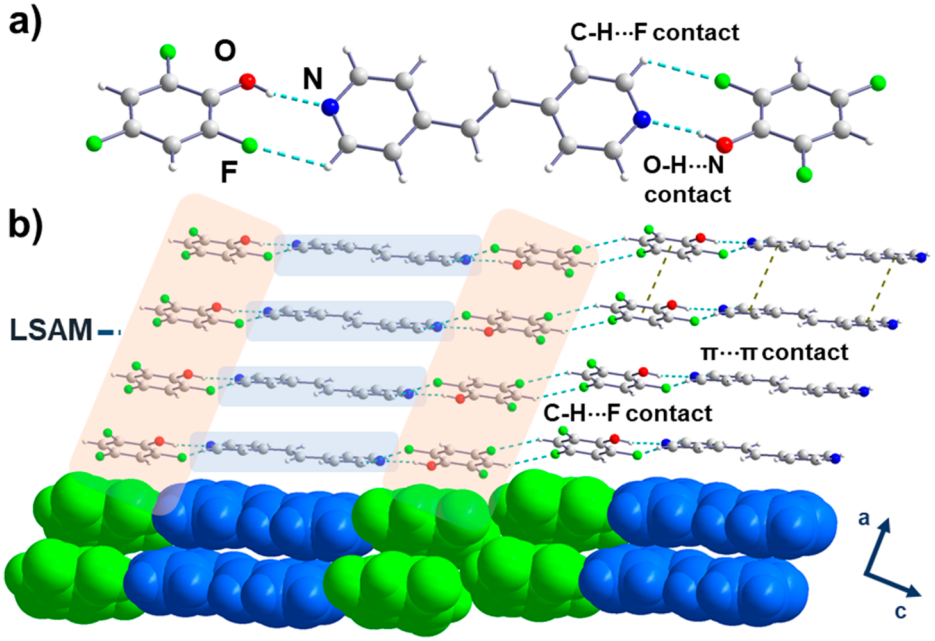

Figure 2. X-ray structure 2(**3F-phOH**)·(**bpe**): (a) hydrogen bonds (O−H···N and C−H···F) and (b) face-to-face π-stacks of **3F-phOH** and **bpe** with LSAM formation (pink).

DOI: 10.1021/acs.cgd.9b00035
Cryst. Growth Des. 2019, 19, 2511−2518

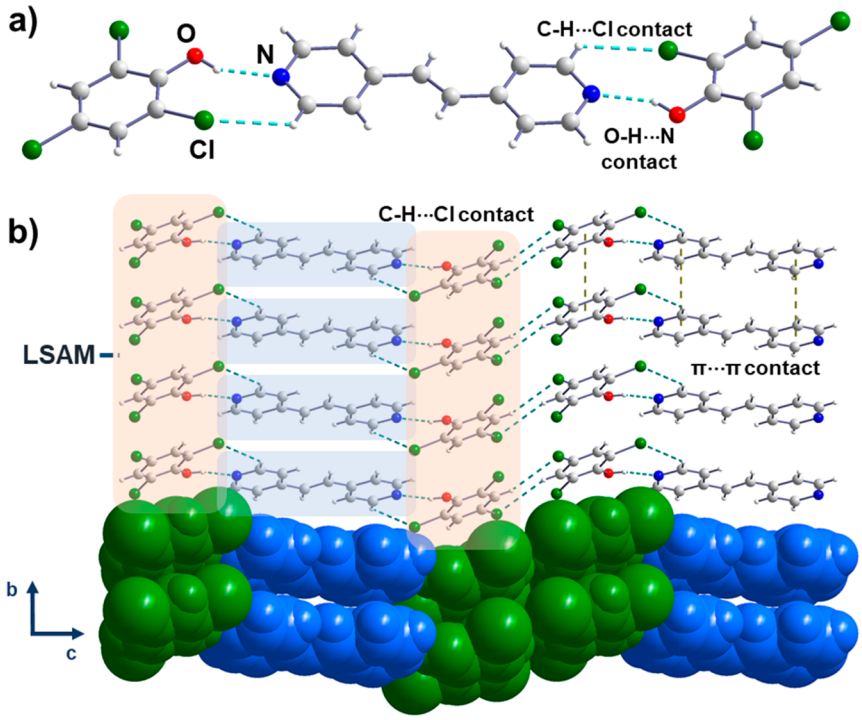

Figure 3. X-ray structure 2(**3Cl-phOH**)·(**bpe**): (a) hydrogen bonds (O−H···N and C−H···Cl) and (b) face-to-face π-stacks of **3Cl-phOH** and **bpe** with LSAM formation (pink).

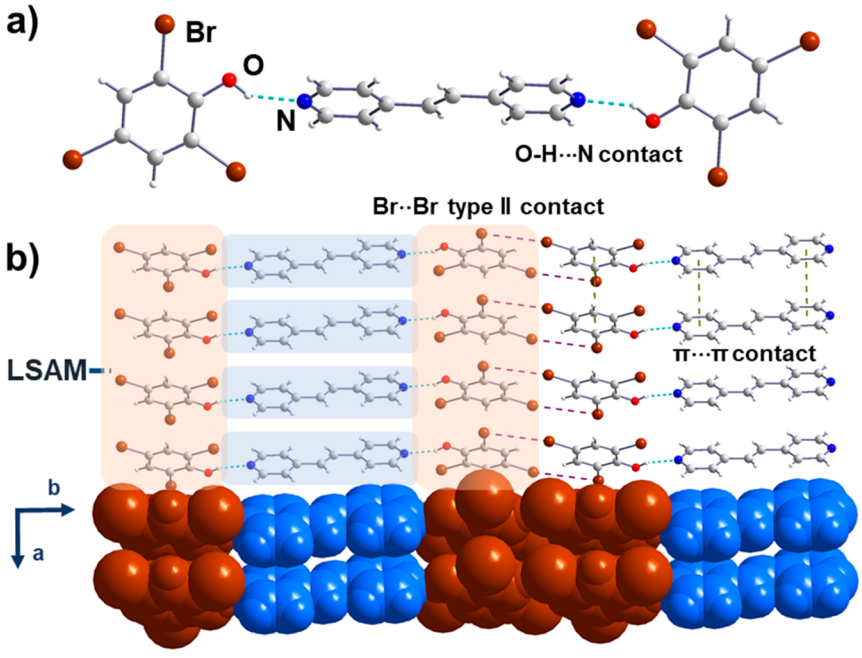

Figure 4. X-ray structure 2(**3Br-phOH**)·(**bpe**): (a) hydrogen bonds (O−H···N) and (b) Br···Br halogen bonds and face-to-face π-stacks of **3Br-phOH** and **bpe** with LSAM formation (pink).

alkene would place the C═C bonds in positions to undergo intermolecular [2 + 2] photodimerizations. The information on the geometry (i.e., stacking distance) and regiochemistry (i.e., hydroxyl group placement) stored in the LSAMs would, thus, orient **bpe** into a geometry suitable for photodimerization.[29]

X-ray Structures. The formation of cocrystals of 2(**3F-phOH**)·(**bpe**), 2(**3Cl-phOH**)·(**bpe**), 2(**3Br-phOH**)·(**bpe**), and 2(**3I-phOH**)·(**bpe**) were confirmed by SCXRD and PXRD, as well as ^{1}H NMR spectroscopy. Despite being identical in composition save for the different halogen atoms, we note that none of the solids were determined to be isostructural due to differences in unit cell parameters and crystal packing.

Coformer **3F-phOH**: The components of 2(**3F-phOH**)·(**bpe**) crystallize in the triclinic space group $P\bar{1}$ to form three-component assemblies sustained by O−H···N hydrogen bonds (Figure 2). In the arrangement, the pyridyl and phenol rings

DOI: 10.1021/acs.cgd.9b00035
Cryst. Growth Des. 2019, 19, 2511−2518

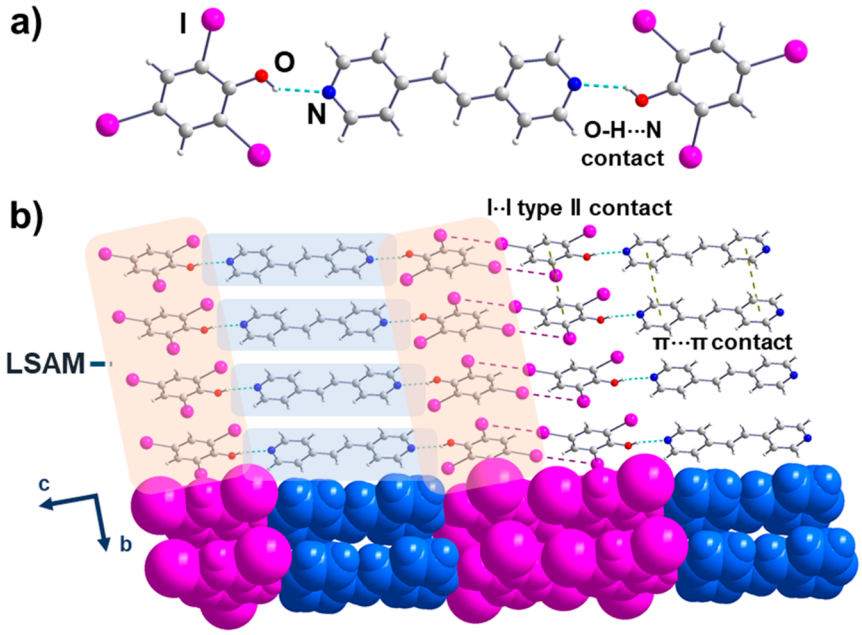

Figure 5. X-ray structure 2(**3I-phOH**)·(**bpe**): (a) hydrogen bonds (O−H···N) and (b) I···I halogen bonds and face-to-face π-stacks of **3I-phOH** and **bpe** with LSAM formation (pink).

Table 2. Photoreactivity Studies of Cocrystals

cocrystal	exposure time (h)	maximum yield of **tpcb** (%)
2(**3F-phOH**)·(**bpe**)	40	96
2(**3Cl-phOH**)·(**bpe**)	110	89
2(**3Br-phOH**)·(**bpe**)	110	76
2(**3I-phOH**)·(**bpe**)	60	no reaction

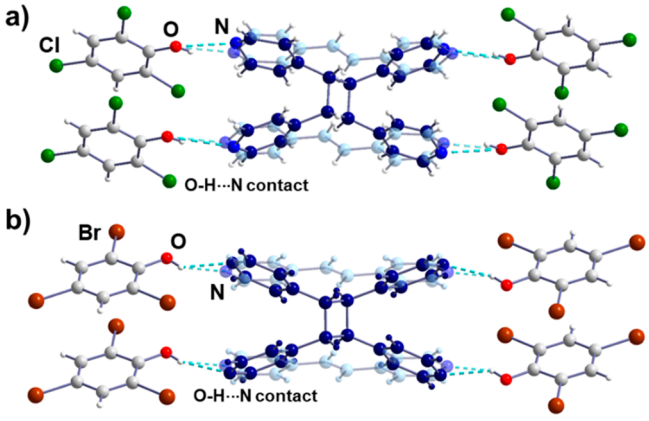

Figure 6. X-ray structures of partial SCSC reactions: (a) 4(**3Cl-phOH**)·(**tpcb**) and (b) 4(**3Br-phOH**)·(**tpcb**).

are twisted from coplanarity (13.6° and 27.8°) (Figure 2a). C−H···F contacts link the assemblies into two-dimensional (2D) sheets that sit within the *bc*-plane (plane shift: 1.45 Å). The sheets stack along the crystallographic *a*-axis with **3F-phOH** and **bpe** participating in infinite face-to-face π-stacks. The stacking of **bpe** preorganizes the C═C bonds parallel and separated by 3.73 Å, which is a geometry suitable for an intermolecular [2 + 2] photodimerization (Figure 2b).[29]

Coformer **3Cl-phOH**: While sheets also form for 2(**3Cl-phOH**)·(**bpe**), the three-component assemblies pack to form a corrugated structure. The components crystallize in the monoclinic space group $P2_1/c$ (Figure 3). The pyridine and phenol rings exhibit a slightly smaller twist (8.0°) compared to 2(**3F-phOH**)·(**bpe**) (Figure 3a). Moreover, the corrugation is manifested along the *c*-axis, being sustained by C−H···Cl[30] forces. The interactions are akin to a hydrophobic zone as described by Desiraju for **3,4-di-X-phenol** (X = Cl, Br).[16] The sheets organize along the *b*-axis (plane shift: 1.99 Å) in face-to-face π-stacks (Figure 3b). The C═C bonds are parallel and separated by 3.98 Å, which also conforms to the postulate of Schmidt.[29]

Coformer **3Br-phOH**: The components of 2(**3Br-phOH**)·(**bpe**) crystallize in the monoclinic space group $P2_1/n$ to form sheets based on three-component assemblies (Figure 4). In contrast to 2(**3F-phOH**)·(**bpe**) and 2(**3Cl-phOH**)·(**bpe**), the sheets are supported by type II halogen bonds[9] ($|\theta_1 - \theta_2|$ = 52.7°) with the phenol and pyridine rings exhibiting a large twist (56.9°) (Figure 4a). Isostructural behavior that may arise owing to the Cl/Br exchange rule[16] is not observed for 2(**3Cl-phOH**)·(**bpe**) and 2(**3Br-phOH**)·(**bpe**). The sheets organize along the *a*-axis (plane shift: 1.92 Å) with the C═C bonds being parallel and separated by 4.04 Å (Figure 4b).[29]

Coformer **3I-phOH**: The components of 2(**3I-phOH**)·(**bpe**) crystallize in the monoclinic space group $P2_1/c$ (Figure 5). The hydrogen-bonded assemblies form corrugated sheets in the *ac*-plane that are supported, similar to 2(**3Br-phOH**)·(**bpe**), by type II I···I halogen bonds[9] ($|\theta_1 - \theta_2|$ = 67.6°) (Figure 5a). In contrast to 2(**3Br-phOH**)·(**bpe**), the phenol and pyridine rings are twisted toward coplanarity (7.4°). The sheets lie offset (plane shift: 2.23 Å) such that the C═C bonds are comparable yet beyond the limit of Schmidt for a photoreaction (4.31 Å) (Figure 5b).[29]

Photoreactivity studies. When powdered crystalline samples of 2(**3X-phOH**)·(**bpe**) (X = F, Cl, Br) were subjected to UV-radiation (medium power Hg lamp) for periods of up to 110 h, the formation of **tpcb** was evidenced by the disappearance of the alkene (7.55 ppm) and appearance of the cyclobutane (4.70 ppm) signals (Table 2). 2(**3I-phOH**)·(**bpe**) was determined to be photostable upon being exposed to UV-radiation for up to 60 h. PXRD analyses before and after

DOI: 10.1021/acs.cgd.9b00035
Cryst. Growth Des. 2019, 19, 2511−2518

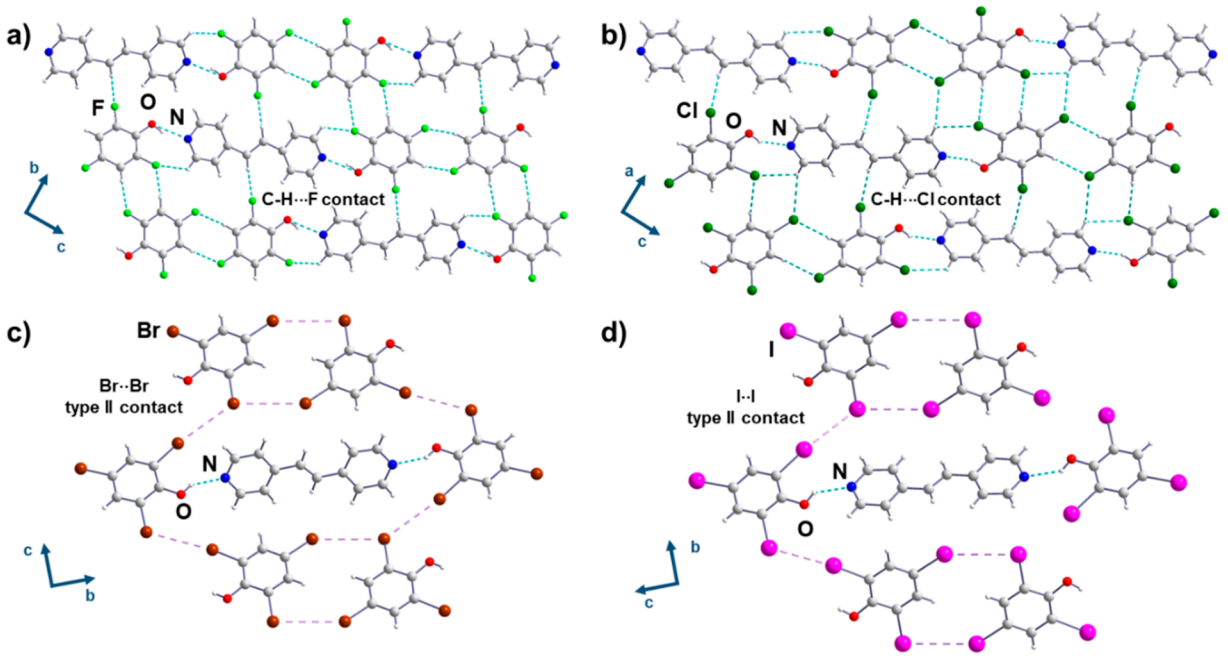

Figure 7. X-ray structures 2(**3X-phOH**)·(**bpe**) showing secondary forces: (a) C−H···F interactions in 2(**3F-phOH**)·(**bpe**), (b) C−H···Cl interactions in 2(**3F-phOH**)·(**bpe**), (c) Br···Br halogen bonds in 2(**3Br-phOH**)·(**bpe**), and (d) I···I halogen bonds in 2(**3I-phOH**)·(**bpe**).

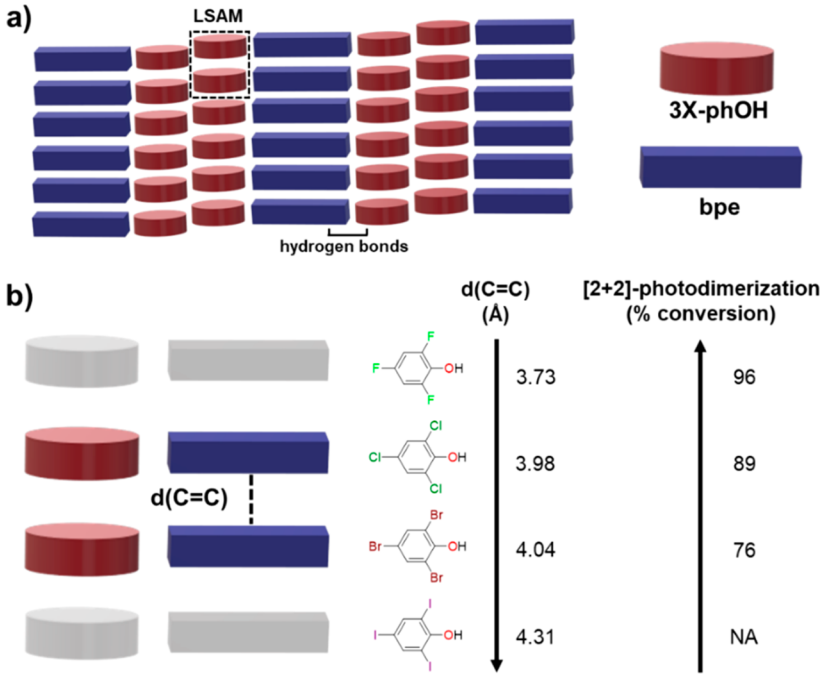

Figure 8. Photoreactivity in cocrystals based on **3X-phOH**: (a) formation of LSAMs and (b) relation of distance with reactivity.

UV-radiation showed each reactive powder to undergo a change in phase following photoreaction (see Supporting Information for PXRD analyses).

Single-Crystal Reactivity. When single crystal samples of 2(**3X-phOH**)·(**bpe**) (X = F, Cl, Br) were irradiated with UV-radiation (gel nail dryer) for 48 h, cocrystals 2(**3Cl-phOH**)·(**bpe**) and 2(**3I-phOH**)·(**bpe**) retained single crystallinity as determined using optical microscopy. Single crystals of 2(**3F-phOH**)·(**bpe**) became opaque and turned to a powder during the same period. SCXRD analyses of the irradiated crystals of 2(**3Cl-phOH**)·(**bpe**) and 2(**3Br-phOH**)·(**bpe**) revealed photodimerizations to occur as partial SCSC transformations to give **tpcb** [yield: 22% (X = Cl) and 42% (X = Br)] (Figure 6). The O−H···N hydrogen bonds were maintained following each photodimerization.[31]

Utility of LSAMs. The LSAMs based on **3X-phOH** that organize **bpe** in the solid state are resilient (Figure 7a−d).[26,27,29] Indeed, 1D stackings of the C═C bonds are maintained despite the presence of secondary interstack interactions in the form of either C−H···X (X = F, Cl) or X···X forces. The resiliency has provided a means, save for X = I, to support photoreactivity of **bpe** in the solid state (Figure

DOI: 10.1021/acs.cgd.9b00035
Cryst. Growth Des. 2019, 19, 2511−2518

8a,b). We note that **tpcb** does not form quantitatively in each case, which is consistent with a model of trapped monomers between dimers.[32,33]

Conclusions. We have introduced the ability of 2,4,6-trihalophenols to direct the [2 + 2] photodimerizations in the solid state. We have shown that long-range assembly properties for **3X-phOH** (X = Cl, I) as pure forms can be transferred to binary cocrystals and, thereby, exploited as LSAMs to achieve the solid-state photoreactions. We are currently studying whether LSAMs based on **3X-phOH** can direct reactivity of more complex alkenes. We are also working to identify other molecules that exhibit similar behavior in the solid state to facilitate the design of photoactive materials with reactivity, as well as unique mechanical, optical. and conductivity properties.

■ ASSOCIATED CONTENT

Supporting Information

The Supporting Information is available free of charge on the ACS Publications website at DOI: 10.1021/acs.cgd.9b00035.

Experimental conditions, ^{1}H NMR spectra, powder X-ray diffractograms, additional SCXRD data, and DSC thermograms (PDF)

Accession Codes

CCDC 1883873−1883878 (for compounds 2(**3F-phOH**)·(**bpe**), 2(**3Cl-phOH**)·(**bpe**), 2(**3Br-phOH**)·(**bpe**), 2(**3I-phOH**)·(**bpe**), 4(**3Cl-phOH**)·(**tpcb**), and 4(**3Br-phOH**)·(**tpcb**)) contain the supplementary crystallographic data for this paper. These data can be obtained free of charge via www.ccdc.cam.ac.uk/data_request/cif, or by emailing data_request@ccdc.cam.ac.uk, or by contacting The Cambridge Crystallographic Data Centre, 12 Union Road, Cambridge CB2 1EZ, UK; fax: +44 1223 336033.

■ AUTHOR INFORMATION

Corresponding Author

*E-mail: len-macgillivray@uiowa.edu. Fax: +1 319-335-1270. Tel: +1 319-335-3504.

ORCID

Gonzalo Campillo-Alvarado: 0000-0002-1868-8523

Leonard R. MacGillivray: 0000-0003-0875-677X

Notes

The authors declare no competing financial interest.

■ ACKNOWLEDGMENTS

We gratefully acknowledge financial support from the National Science Foundation (DMR-1708673) and the Mexican National Council for Science and Technology (CONACYT).

■ REFERENCES

(1) Ganguly, P.; Desiraju, G. R. Long-range synthon Aufbau modules (LSAM) in crystal structures: systematic changes in $C_6H_{6-n}F_n$ ($0 \leq n \leq 6$) fluorobenzenes. *CrystEngComm* **2010**, *12*, 817−833.

(2) Thakur, T. S.; Sathishkumar, R.; Dikundwar, A. G.; Guru Row, T. N.; Desiraju, G. R. Third Polymorph of Phenylacetylene. *Cryst. Growth Des.* **2010**, *10*, 4246−4249.

(3) Mukherjee, A.; Desiraju, G. R. Halogen Bonding and Structural Modularity in 2,3,4- and 3,4,5-Trichlorophenol. *Cryst. Growth Des.* **2011**, *11*, 3735−3739.

(4) Dikundwar, A. G.; Sathishkumar, R.; Guru Row, T. N.; Desiraju, G. R. Structural Variability in the Monofluoroethynylbenzenes Mediated through Interactions Involving "Organic" Fluorine. *Cryst. Growth Des.* **2011**, *11*, 3954−3963.

(5) Mukherjee, A.; Dixit, K.; Sarma, S. P.; Desiraju, G. R. Aniline−phenol recognition: from solution through supramolecular synthons to cocrystals. *IUCrJ* **2014**, *1*, 228−239.

(6) Dubey, R.; Mir, N. A.; Desiraju, G. R. Quaternary cocrystals: combinatorial synthetic strategies based on long-range synthon Aufbau modules (LSAM). *IUCrJ* **2016**, *3*, 102−107.

(7) Paul, M.; Chakraborty, S.; Desiraju, G. R. Six-Component Molecular Solids: ABC$[D_{1-(x+y)}E_xF_y]2$. *J. Am. Chem. Soc.* **2018**, *140*, 2309−2315.

(8) Desiraju, G. R. Crystal Engineering: From Molecule to Crystal. *J. Am. Chem. Soc.* **2013**, *135*, 9952−9967.

(9) Mukherjee, A.; Tothadi, S.; Desiraju, G. R. Halogen bonds in crystal engineering: like hydrogen bonds yet different. *Acc. Chem. Res.* **2014**, *47*, 2514−2524.

(10) Mukherjee, A. Building upon Supramolecular Synthons: Some Aspects of Crystal Engineering. *Cryst. Growth Des.* **2015**, *15*, 3076−3085.

(11) Campillo-Alvarado, G.; Brannan, A. D.; Swenson, D. C.; MacGillivray, L. R. Exploiting the Hydrogen-Bonding Capacity of Organoboronic Acids to Direct Covalent Bond Formation in the Solid State: Templation and Catalysis of the [2 + 2] Photodimerization. *Org. Lett.* **2018**, *20*, 5490−5492.

(12) Ericson, D. P.; Zurfluh-Cunningham, Z. P.; Groeneman, R. H.; Elacqua, E.; Reinheimer, E. W.; Noll, B. C.; MacGillivray, L. R. Regiocontrol of the [2 + 2] Photodimerization in the Solid State Using Isosteric Resorcinols: Head-to-Tail Cyclobutane Formation via Unexpected Embraced Assemblies. *Cryst. Growth Des.* **2015**, *15*, 5744−5748.

(13) Campillo-Alvarado, G.; Aslan, K.; Sinnwell, M. A.; Reinheimer, E. W.; Mariappan, S. S.; Macgillivray, L. R.; Groeneman, R. H. A solid-state [2+ 2] photodimerization involving coordination of Ag (I) ions to 2-pyridyl groups. *J. Coord. Chem.* **2018**, *71*, 2875−2883.

(14) MacGillivray, L. R.; Papaefstathiou, G. S.; Friščić, T.; Hamilton, T. D.; Bučar, D.-K.; Chu, Q.; Varshney, D. B.; Georgiev, I. G. Supramolecular Control of Reactivity in the Solid State: From Templates to Ladderanes to Metal−Organic Frameworks. *Acc. Chem. Res.* **2008**, *41*, 280−291.

(15) Chaudhary, A.; Mohammad, A.; Mobin, S. M. Recent Advances in Single-Crystal-to-Single-Crystal Transformation at the Discrete Molecular Level. *Cryst. Growth Des.* **2017**, *17*, 2893−2910.

(16) Mukherjee, A.; Desiraju, G. R. Halogen bonds in some dihalogenated phenols: applications to crystal engineering. *IUCrJ* **2014**, *1*, 49−60.

(17) Aung, T.; Liberko, C. A. Bringing photochemistry to the masses: A simple, effective, and inexpensive photoreactor, right out of the box. *J. Chem. Educ.* **2014**, *91*, 939−942.

(18) Sheldrick, G. M. SHELXT−Integrated space-group and crystal-structure determination. *Acta Crystallogr., Sect. A: Found. Adv.* **2015**, *71*, 3−8.

(19) Sheldrick, G. M. Crystal structure refinement with SHELXL. *Acta Crystallogr., Sect. C: Struct. Chem.* **2015**, *71*, 3−8.

(20) Dolomanov, O. V.; Bourhis, L. J.; Gildea, R. J.; Howard, J. A.; Puschmann, H. OLEX2: a complete structure solution, refinement and analysis program. *J. Appl. Crystallogr.* **2009**, *42*, 339−341.

(21) Farrugia, L. J. WinGX suite for small-molecule single-crystal crystallography. *J. Appl. Crystallogr.* **1999**, *32*, 837−838.

(22) Vetter, W. Marine halogenated natural products of environmental relevance. In *Reviews of Environmental Contamination and Toxicology*; Springer: 2006; pp 1−57.

(23) Lu, J.; Shao, J.; Liu, H.; Wang, Z.; Huang, Q. Formation of halogenated polyaromatic compounds by laccase catalyzed transformation of halophenols. *Environ. Sci. Technol.* **2015**, *49*, 8550−8557.

(24) Metrangolo, P.; Resnati, G. Type II halogen··· halogen contacts are halogen bonds. *IUCrJ* **2014**, *1*, 5−7.

(25) Reddy, C. M.; Gundakaram, R. C.; Basavoju, S.; Kirchner, M. T.; Padmanabhan, K. A.; Desiraju, G. R. Structural basis for bending of organic crystals. *Chem. Commun.* **2005**, 3945−3947.

(26) Gonzalez Martinez, S. P.; Bernes, S. 2,4,6-Trichlorophenol. *Acta Crystallogr., Sect. E: Struct. Rep. Online* **2007**, *63*, o3947.
(27) Nath, N. K.; Saha, B. K.; Nangia, A. Isostructural polymorphs of triiodophloroglucinol and triiodoresorcinol. *New J. Chem.* **2008**, *32*, 1693−1701.
(28) Brock, C. P.; Duncan, L. L. Anomalous space-group frequencies for monoalcohols CnHmOH. *Chem. Mater.* **1994**, *6*, 1307−1312.
(29) Schmidt, G. Photodimerization in the solid state. *Pure Appl. Chem.* **1971**, *27*, 647−678.
(30) Aakeröy, C. B.; Evans, T. A.; Seddon, K. R.; Pálinkó, I. The C−H···Cl hydrogen bond: does it exist? *New J. Chem.* **1999**, *23*, 145−152.
(31) Sinnwell, M. A.; Blad, J. N.; Thomas, L. R.; MacGillivray, L. R. Structural flexibility of halogen bonds showed in a single-crystal-to-single-crystal [2 + 2] photodimerization. *IUCrJ* **2018**, *5*, 491−496.
(32) Wernick, D. L.; Schochet, S. Kinetics of dimerization in stack crystal structures. *J. Phys. Chem.* **1988**, *92*, 6773−6778.
(33) Desiraju, G. R.; Kannan, V. What is the maximum yield in the solid state cinnamic acid dimerisation? A combinatorial mathematical approach. *Proc. - Indian Acad. Sci., Chem. Sci.* **1986**, *96*, 351−362.

DOI: 10.1021/acs.cgd.9b00035
Cryst. Growth Des. 2019, 19, 2511−2518